Water Diffusion in Glassy Polymers and their Silica Hybrids: an Analysis of State of Water Molecules and of the Effect of Tensile Stress

Domenico Larobina,[1] *Marino Lavorgna,*[1] *Giuseppe Mensitieri,*[*2] *Pellegrino Musto,*[3] *Alain Vautrin*[4]

Summary: In-situ, time-resolved FTIR spectroscopy along with gravimetric analysis have been used to investigate water sorption and transport in several glassy polymeric matrices, characterized by different levels of interaction with water, as well as on polymer-silica hybrids. This technique has also been coupled to a dynamical-mechanical analyser to gather information on the water sorption kinetics and thermodynamics in a polymer sample submitted to stretching deformation and load. Results have been modelled by coupling the mass balance and momentum balance, using a theoretical approach developed for elastic matrices and low sorbed amounts by Larché and Cahn.

Keywords: diffusion; epoxy; FT-IR; polyimides; stress

Introduction

Mass transport of low molecular weight compounds in polymeric materials has a great scientific and technological interest with reference to durability of high performance matrices for composites. In fact these matrices, when exposed to humid environments, absorb significant amounts of water which adversely affects their physical-mechanical properties. The main documented effects are, among others, plasticization, changes of physical properties, hygrothermal degradation and swelling stresses. To explain the anomalous sorption features of some glassy polymers several authors have proposed that the water is made up of two species, i.e., those forming a molecular solution and those confined into areas of abnormally large free volume, often referred to as microvoids.[1] Several investigations on difunctional epoxies based on dielectric relaxation spectroscopy (DRS) and combined DRS and FTIR measurements support the idea of water molecules partly bound to polymer chains and partly clustered into microvoids.[2,3] In-situ, time-resolved FTIR spectroscopy provides not only a means for monitoring accurately the penetrant sorption kinetics and equilibrium sorption isotherm, but also offers the possibility of investigating in detail the concurrent development of molecular interactions.[4] In the present contribution this technique has been used to investigate water sorption and transport properties in a) three high performance polymer matrices characterized by different levels of interaction with water, i.e. TGDDM-DDS and TGDDM-HHPA epoxy resins and PMDA-ODA polyimide and b) an inorganic-organic silica-polyimide hybrid. In-situ, time-resolved FTIR spectroscopy has also been coupled to a dynamical-mechanical

[1] Institute for Composite and Biomedical Materials, National Research Council (IMCB-CNR), P.le E. Fermi 1, Portici, Naples, Italy
[2] Department of materials and Production Engineering, University of Naples Federico II, P.le Tecchio, 80125, Naples, Italy
E-mail: mensitie@unina.it
[3] Institute for Chemistry and Technology of Polymers, National Research Council (ICTP-CNR), via Campi Flegrei 34, 80078 Pozzuoli, Naples, Italy
[4] Ecole Nationale Supérieure des Mines de Saint-Etienne, 158,cours Fauriel, 42023 SAINT-ETIENNE cedex 2, FRANCE

Copyright © 2007 WILEY-VCH Verlag GmbH & Co. KGaA, Weinheim

analyser to gather information on the water sorption kinetics and thermodynamics in polyimide submitted to stretching deformation and load.

Experimental Part

Materials

- The epoxy resins investigated were prepared starting from: a) a commercial grade tetraglycidyl-4,4′ diamino diphenylmethane (TGDDM) supplied by Ciba Geigy (Basel, Switzerland), and the curing agent was 4,4′-diamino-diphenylsulphone (DDS) from Aldrich (Milwaukee, WI). Thin films were obtained [thickness = 9 ± 0.5 μm]; b) a commercial grade tetraglycidyl-4,4′ diaminodiphenylmethane (TGDDM) supplied by Ciba Geigy (Basel, Switzerland), and the curing agent was hexa-hydrophtalic-anhydride (HHPA) from Sigma-Aldrich Italy (Milan, Italy). Thin films were obtained [thickness (L) = 22 ± 0.5 μm
- The polyimide was a condensation product of pyromellitic dianhydride (PMDA) and oxydianiline (ODA). Thin films (about 20 μm thick) were obtained from a poly(amic acid) solution (14 wt %) in N-methyl pyrrolidone and xylene (trade name Pyre ML RK692 from DuPont, Wilmington, DE). The achievement of full imidization of the amic acid was confirmed spectroscopically
- To obtain polyimide-silica hybrids, 3.46 g of tetraethoxysilane TEOS, 0.86 g EtOH, 1.20 g γ-glycidyloxypropyltrimethoxysilane GOTMS, 082 g H_2O and 0.12 g aqueous HCl solution (2.0 wt %) were added sequentially in a glass vial. The precursor hybrid solution was subsequently obtained by adding dropwise the hydrolysed alkoxysilane solution to the polyamic acid solution (the same adopted for PMDA-ODA synthesis). The precursors solution was then cast on glass slides and kept at 80 °C for 1 hour to allow most of the solvent to evaporate. Imidization and condensation reactions were carried out in successive isothermal steps at increasing temperature up to 300 °C.

Water Sorption Analysis by in-situ, Time-Resoved FTIR Spectroscopy and Gravimetry

A vacuum tight FT-IR cell was designed to monitor the FT-IR transmission spectra of the polymer films exposed to a controlled humidity environment. Tests were performed at several activity levels of water vapour at 24 °C on epoxies and at 30 °C on polyimide and polyimide-silica hybrids. The cell has been properly modified to perform, during the FTIR analysis, also mechanical and dynamical-mechanical tests (tensile) on samples. Subtraction spectroscopy was performed on the spectra of 'dry' resin and resin containing absorbed water, investigating the ν_{OH} region. To determine weight gain of samples exposed to a controlled humidity environment, an electronic microbalance was used (D200, CAHN Instruments, Madison, WI, sensitivity 0.1 μg).

Results and discussion

Water Sorption in TGDDM-DDS and TGDDM-HHPA

The in-situ FTIR analysis coupled to gravimetric analysis allowed the evaluation of concentration of different types of water molecules sorbed in the polymeric matrices both at sorption equilibrium and during sorption tests. Here the different water species are selectively identified as S_0, S_1 and S_2 species on the basis of the number of H-bonds they form with proton acceptor groups, which, in turn, are indicated by the subscripts 0, 1, and 2. The different interactional capability of the matrices with water molecules is reflected in very different relative contributions of the water populations. Towards a quantitative assessment of the water species populations, an analysis has been perfomed to evaluate molar absorptivities of each water species, starting from the knowledge of molar absorptivity of S_0 species. In fact the shift of the ν_{O-H} peak , $\Delta\nu$, has been reported to be quantitatively related to the intensity change, $\Delta\varepsilon$. In particular, Huggins and Pimentel[5] and, later, Mirone and Fabbri[6],

Copyright © 2007 WILEY-VCH Verlag GmbH & Co. KGaA, Weinheim

reported a relatively simple relationship between these two spectral parameters for several H-bonding binary systems, which is generally applicable to a wide variety of donor-acceptor pairs. The $\Delta\nu$–$\Delta\varepsilon$ correlation affords an estimation of the absorptivity values of the different water species present in the system under investigation. This estimation was performed as follows: Previous studies made by us on the TGDDM-DDS system using NIR spectroscopy[7,8] allowed us to evaluate the ratio C_{S_0}/C as a function of the total weight concentration of absorbed water, as evaluated gravimetrically (here C and C_{S_0}represent, respectively, the total concentration of sorbed water and the concentration of S_0 species, both expressed mol cm^{-3}). The linear relationship interpolating these data has been used to evaluate, in the present experimental conditions, C_{S_0} from the gravimetric sorption data. Then, the reduced absorbance (A/L, where L is the film thickness) of the S_0 peak at 3623 cm^{-1} when plotted versus the C_{S_o} values, obtained at sorption equilibrium at the four investigated activities, displays a linear correlation passing through the origin, as predicted by the Beer-Lambert relationship. The slope of the best fitting straight line provides the value of the molar absorptivity of unassociated water (ε_{S_0}) expressed in cm mol^{-1}. Subsequently, the molar absorptivity enhancement, $\Delta\varepsilon_{s_i}$for each species, relative to the reference state (S_0) was evaluated from the $\Delta\nu$–$\Delta\varepsilon$ relationship[5] and was transformed in the absolute value of $\varepsilon_{s_i}$by adding $\varepsilon_{S_0}$to $\Delta\varepsilon_{s_i}$. A similar approach was adopted for the case of TGDDM-HHPA. The knowledge of the absorptivities of the various water species allows us to transform the absorbance into concentration values according to:

$$C = C_{S_0} + C_{S_1} + C_{S_2} = \frac{1}{\mathrm{L}}\left(\frac{A_{S_0}}{\varepsilon_{s_0}} + \frac{A_{S_1}}{\varepsilon_{S_1}} + \frac{A_{S_2}}{\varepsilon_{S_2}}\right) \quad (1)$$

According to this procedure, a fully spectroscopic estimate of the total concentration of absorbed water and of the concentration of each species can be obtained. For TGDDM-DDS and TGDDM-HHPA an excellent agreement was found between the gravimetric and FT-IR spectroscopy values of the total concentration of water absorbed at equilibrium at the four investigated activities. The higher interactive nature towards water molecules of TGDDM-DDS is demonstrated in Figure 1 where it is evident the higher relative amount of non-interacting water species at sorption equilibrium in the case of TGDDM-HHPA as compared to TGDDM-DDS. The different level of interaction is also reflected in the higher sorption capacity of the TGDDM-DDS (see sorption isotherms in Figure 2). Another important information gathered from the analysis of spectroscopic results is the establishment of a *linear instantaneous local equilibrium* among the different sorbed water species. This result is fundamental in the development of the model adopted for the interpretation of sorption kinetics. For both TGDDM-DDS and TGDDM-HHPA water sorption kinetics is faster than desorption, indicating that water diffusivity is an increasing function of concentration,[9] the sorption-desorption lag being more pronounced for the TGDDM-DDS resin, pointing to a stronger dependence of sorption kinetics on water concentration than for TGDDM-HHPA. This concentration dependence is also evident when considering the sorption experiments performed at different activities:

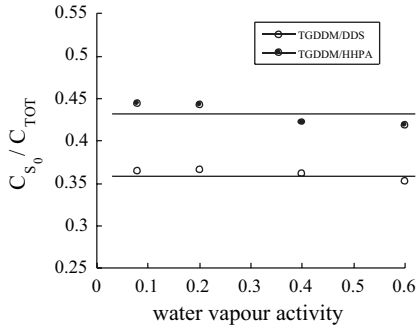

Figure 1.
Relative amount of S_0 species at sorption equilibrium vs water activity

Copyright © 2007 WILEY-VCH Verlag GmbH & Co. KGaA, Weinheim

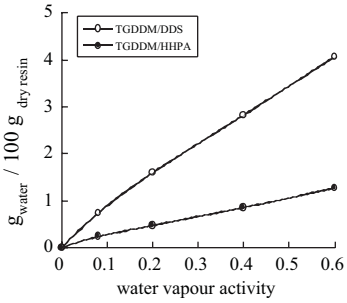

Figure 2.
Gravimetric water sorption isotherms for the two epoxies at 24 °C.

for both resins the sorption rate, and consequently the effective diffusivity, increases with water activity. Again, this effect is more pronounced in the case of the TGDDM-DDS system.

In interpreting sorption kinetics, it should be considered that the molecular mechanisms involved in the transport are: 1) diffusion of water molecules through the polymer matrix, which is concentration dependent due to the free volume increase associated with solubilization 2) interactions of water molecules with specific sites distributed on the polymer network, that slow down the diffusion process. As discussed in a previous paper on TGDDM-DDS,[4] this latter effect could be modeled by assuming that diffusion is associated with the reversible formation of molecular aggregates between water molecules and interaction sites. In view of the experimental results, which points for both TGDDM-DDS and TGDDM-HHPA to the establishment of an *instantaneous local equilibrium* among the various water species, it has been further assumed that a Langmuir-type absorption mechanism relates the concentration of 'free' water molecules (C_{S_0}) and the concentration of 'bound' water molecules (C_{S_1} and C_{S_2}):

$$C_{S_i} = \frac{K_i \cdot C_{S_0} \cdot C_i^0}{1 + K_i \cdot C_{S_0}} \tag{2}$$

where K_i are taken as constants and C_i^0 is the total concentration of sites of type i available on the backbone. Furthermore, the model is based on the presumption that water molecules involved in these interactions have a negligible mobility as compared to 'free' water molecules, obtaining:

$$\phi^{-1} \cdot \frac{\partial C_{S_0}}{\partial t} = \frac{\partial}{\partial x}\left(D(C)\frac{\partial C_{S_0}}{\partial x}\right) \tag{3}$$

with:

$$\phi^{-1} = 1 + \frac{C_1^0 \cdot K_1}{(1 + K_1 \cdot C_{S_0})^2} + \frac{C_2^0 \cdot K_2}{(1 + K_2 \cdot C_{S_0})^2} \tag{4}$$

Here C is the total concentration of sorbed water (i.e. $C_{S_0} + C_{S_1} + C_{S_2}$). The 'interaction factor', ϕ, if the *instantaneous local equilibrium* established among the various water species is *linear*, as experimentally observed in both the epoxy systems, assumes a particularly simple form, which is independent on water concentration:

$$\phi = \left(1 + \sum_{i=1}^{n} K_i C_i^0\right)^{-1} = \left(1 + \sum_{i=1}^{n} \frac{C_{S_i}}{C_{S_0}}\right)^{-1} \tag{5}$$

Since the adopted Langmuir-type absorption model is non-linear, the experimentally observed establishment of a linear equilibrium among the different water species should be concurrently accompanied by the further condition that the interacting sites of the resins are far from being saturated. In fact, at a sufficiently low concentration of sorbant, Langmuir-type isotherms approach linearity. On the basis of the results of spectroscopic analysis and of stoichiometric evaluations this is actually the case for the systems at hand. As a consequence of the independence of ϕ on concentrantion, we can write:

$$\frac{\partial C_{S_0}}{\partial t} = \frac{\partial}{\partial x}\left(\phi \cdot D(C)\frac{\partial C_{S_0}}{\partial x}\right) \tag{6}$$

Moreover, since for the linearity of the adsorption equilibrium we have:

Copyright © 2007 WILEY-VCH Verlag GmbH & Co. KGaA, Weinheim

$C_{S_i} = C_0^i \cdot K_i \cdot C_{S_0}$ and $C = C_{S_0} + C_{S_1} + C_{S_2} = C_{S_0} \cdot (1 + K_1 \cdot C_1^0 + K_2 \cdot C_2^0)$, consequently:

$$\frac{\partial C_{S_i}}{\partial t} = \frac{\partial}{\partial x}\left(\phi \cdot D(C)\frac{\partial C_{S_i}}{\partial x}\right) \quad (7)$$

and

$$\frac{\partial C}{\partial t} = \frac{\partial}{\partial x}\left(\phi \cdot D(C)\frac{\partial C}{\partial x}\right) = \frac{\partial}{\partial x}\left(D_{eff}(C)\frac{\partial C}{\partial x}\right) \quad (8)$$

The effective mutual diffusivity coefficient, $D_{eff}(C)$, which characterizes the overall sorption kinetics, can be factorized as the product of i) a contribution consisting of a concentration dependent mutual diffusivity, $D(C)$, which takes into account free volume changes and would characterize transport through the material in the absence of the 'sticking' effect due to the molecular interactions, and ii) a 'interaction' factor, ϕ, which accounts for the interaction with specific sites:

$$D_{eff}(C) = (C) \cdot \phi \quad (9)$$

It is worth noting that ϕ accounts for the direct effect of interactions on the diffusive movements of water molecules. Actually, establishment of water/epoxy interactions indirectly affects also $D(C)$, since it is reasonable that these interactions do perturb the network structure as well. From the spectroscopic data, ϕ has been calculated to be equal to 0.35 and 0.45 for the TGDDM-DDS and TGDDM-HHPA resins, respectively. The lower value of ϕ for the TGDDM-DDS resin, reflects the higher interaction energy of the specific sites present on the network (amino-alcohol and sulphonic groups) as compared to the case of TGDDM-HHPA (ester carbonyls). An estimate of $D_{eff}(C)$ for both resins can be obtained from the integral sorption curves (spectroscopic data in the from the ν_{OH} band) determined at different water vapour activities, by applying a well established procedure.[9] In Table 1 are summarized the results obtained for both resins, which show that both D_{eff} and D are increasing functions of concentration. The analysis of these results indicates that the TGDDM-DDS resin displays lower values for $D(C)$ and its value is also more sensitive to water concentration (see relative changes in $D(C)$). This points to a network structure which is more tightly packed than in the case of TGDDM-HHPA and, consequently, more sensitive to free volume changes associated with water sorption which perturbs the molecular structure of the polymer network. The presence of stronger interactive sites, which determine a lower value of ϕ, contributes to a further decrease of the effective diffusivity, related to the 'sticking' of water molecules on these sites. The consequence are lower values of $D_{eff}(C)$ and a higher dependence on water concentration.

Water Sorption in Polyimides and Polyimide-Silica Hybrids

The normalised absorbance of the ν_{OH} water band is considerably higher in the hybrid than in pure polyimide, suggesting that there is a higher amount of sorbed water in the system. At the same time, there is a considerably higher contribution to H-bonding from strongly interacting species. This can be explained considering that the silica domains in the nanocomposite system contain a large amount of surface OH groups, which promote strong

Table 1.
Equilibrium water content, diffusivities and interaction factors for the sorption tests performed at different activities on the TGDDM-DDS and TGDDM-HHPA resins.

TGDDM-DDS				TGDDM-HHPA			
C_0 [% *b.w.*]	$D_{eff}(C)$ [cm^2/s]	$D(C)$ [cm^2/s]	ϕ	C_0 [% *b.w.*]	$D_{eff}(C)$ [cm^2/s]	$D(C)$ [cm^2/s]	ϕ
0.75	$3.65 \cdot 10^{-10}$	$10.4 \cdot 10^{-10}$	0.35	0.26	$2.07 \cdot 10^{-9}$	$4.6 \cdot 10^{-9}$	0.45
1.61	$5.48 \cdot 10^{-10}$	$15.7 \cdot 10^{-10}$	0.35	0.49	$2.13 \cdot 10^{-9}$	$4.73 \cdot 10^{-9}$	0.45
2.83	$8.06 \cdot 10^{-10}$	$23.0 \cdot 10^{-10}$	0.35	0.87	$2.25 \cdot 10^{-9}$	$5.00 \cdot 10^{-9}$	0.45
4.07	$10.7 \cdot 10^{-10}$	$30.6 \cdot 10^{-10}$	0.35	1.28	$2.37 \cdot 10^{-9}$	$5.27 \cdot 10^{-9}$	0.45

Copyright © 2007 WILEY-VCH Verlag GmbH & Co. KGaA, Weinheim

H-bonding interactions. In the case of the hybrid the relative contributions (at sorption equilibrium) of S_0, S_1 and S_2 species are slightly dependent on water activity. Conversely, significant changes are observed for pure polyimide. In both cases, however, the relative concentration of S_2 species increases with total concentration of absorbed water. For the case of pure polyimide this effect may be related to the tendency of water to form clusters. On the other hand, for the case of the hybrid this is likely to be due to the fact that, at the levels of water activity used in the experiments, the adsorption of water molecules on the interacting sites of the inorganic phase is far from the saturation conditions. In terms of absorbance areas, the S_2 species within the hybrid have a higher absorbance (by almost one order of magnitude), than those of S_0 and S_1, whereas for pure polyimide comparable values of the relative absorbance areas are found. This confirms the much stronger interactive character of the hybrid system, resulting from the presence of the inorganic domains. Gravimetric sorption isotherms , (see Figure 3) are consistent with this interpretation, not only because the solubility of water in the hybrid is higher but also in view of the significant difference in the shape of the isotherms. The slight downward concavity of the isotherm in the case of the nanocomposite, points to the presence of water adsorbed on specific sites within the inorganic phase.

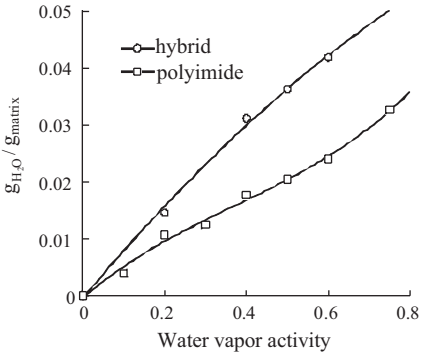

Figure 3.
Gravimetric water sorptio isotherms at 30 °C for PMD-ODA and the hybrid.

Effect of Tensile Stress on Water Sorption in Polyimide

Water vapor sorption kinetics, at an activity equal to 0.3 and at a temperature of 30 °C, have been determined for unloaded, constant loaded and constant deformed thin films using on-line FTIR spectroscopy (see Scheme 1). In view of the non-Fickian behavior of sorption kinetics, supposed to be related to the effect of stresses associated with water penetration, data have been interpreted using the network theory of interstitial solutions proposed by Larchè and Cahn[10] for diffusion of low molecular weight solutes in solids.

The original approach, developed for solid samples free from externally imposed loads or deformation, accounts for the effect, on the solute diffusion process, of the stress field induced as a consequence of the profile of swelling dilation. The solid is assumed to behave elastically. The field equations of the model are the solute mass balance, the force balance and the compatibility condition for the total deformation which are coupled through the dependence of the solute chemical potential on concentration and on the state of stress, as well as through the dependence of the stress state upon solute concentration. In the limit of small deformations, low solute concentration and negligible effect of body forces,

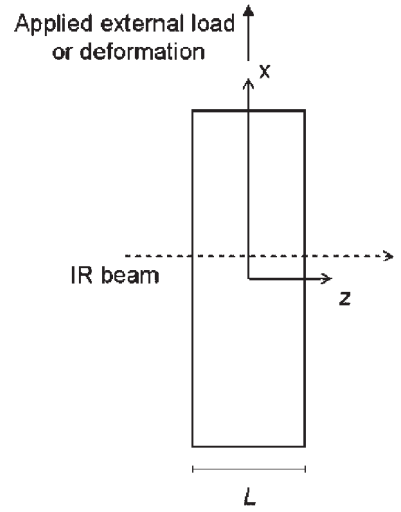

Scheme 1.

Copyright © 2007 WILEY-VCH Verlag GmbH & Co. KGaA, Weinheim

the relevant equations, for the case of a sorption experiment in a thin film, are[11]:

$$\frac{1}{V_1}\frac{\partial \varphi}{\partial t} = -\frac{\partial}{\partial z} J_z \tag{10}$$

$$\nabla \cdot \underline{\underline{T}} = 0 \tag{11}$$

$$\nabla \mathbf{x} \underline{\underline{E}} \mathbf{x} \nabla = \mathbf{0} \tag{12}$$

Here it has been assumed that stress field equilibrates instantaneously as compared to the composition field. The mass flux, J_z, has been taken to be equal to:

$$J_z = -\frac{D\varphi}{V_1 RT} \cdot \frac{\partial \mu}{\partial \varphi} \cdot \frac{\partial \varphi}{\partial z} \tag{13}$$

In the previous expressions ϕ is the solute volume fraction, V_1 is the solute partial molar volume, $\underline{\underline{T}}$ is the Cauchy stress tensor, $\underline{\underline{E}}$ is the strain tensor and D is the thermodynamic diffusivity, which is assumed to be not dependent on solute concentration and on the state of stress. The total strain tensor ($\underline{\underline{E}}$) is the sum of the contribution of the swelling strain tensor ($\underline{\underline{E}}^c$) and of the mechanically induced strain tensor ($\underline{\underline{E}}^m$):

$$\underline{\underline{E}} = \underline{\underline{E}}^c + \underline{\underline{E}}^m \tag{14}$$

A constitutive equation for the Cauchy stress tensor have to be assigned in the form:

$$\underline{\underline{T}} = f(\underline{\underline{E}}^m) \tag{15}$$

This relationship, in the framework of the linear theory of Larchè and Cahn for isotropic solids, is the Young's law. Assuming that $d\underline{\underline{E}}^c \big/ d\varphi$ is constant[10], we have:

$$\underline{\underline{E}}^c = \eta \cdot \varphi \cdot \underline{\underline{I}} \tag{16}$$

where η is the appropriate constant coefficient of linear expansion. In the cases in which the variation of elastic coefficients with composition is negligible, the solute chemical potential can be demonstrated to be given by the following expression[12]:

$$\mu(\underline{\underline{T}}, \varphi) = \mu(\underline{\underline{0}}, \varphi) - \eta \cdot V_1 \cdot tr(\underline{\underline{T}}) \tag{17}$$

The $tr(\underline{\underline{T}})$ term depends on geometry of the sample and on the type of boundary conditions. In general it contains integrals, over the sample volume, of the solute volume fraction. As a consequence, the chemical potential and, in turn, the mass flux at a point in the material are non-local function of the solute volume fraction, since their value is also dependent upon the overall volume fraction profile. This is a distinctive feature as compared to the simple case of the classical Fickian diffusion behavior. For the particular case of a free standing thin film with symmetrical boundary conditions, it is obtained[10,13]:

$$tr(\underline{\underline{T}}) = \frac{2\eta E}{(1-\nu)}\left[-\varphi + \frac{1}{L}\int_{-L/2}^{L/2} \varphi dz\right] \tag{18}$$

$$J_z = -\frac{D}{V_1}\left[1 + \frac{\partial \ln \gamma}{\partial \ln \varphi} + \frac{2\eta^2 V_1 E}{RT(1-\nu)}\right]\frac{\partial \varphi}{\partial z} \tag{19}$$

where ν is the Poisson's ratio and γ is the solute activity coefficient. As is evident, for such a case, the mass flux depends only upon local values. If ideal thermodynamic behavior can be assumed for $\mu(\underline{\underline{0}}, \varphi)$, the expression for J_z becomes:

$$J_z = -\frac{D}{V_1}\left[1 + \frac{2\eta^2 V_1 E\varphi}{RT(1-\nu)}\right]\frac{\partial \varphi}{\partial z} = -\frac{D_{eff}}{V_1}\frac{\partial \varphi}{\partial z} \tag{20}$$

where D_{eff} is an 'effective' diffusion coefficient. If the thin film is submitted to a constant external tensile load (F_x) or constant total deformation (E_x^{TOT}) in the x direction the expression for $tr(\underline{\underline{T}})$ become, respectively:

$$tr(\underline{\underline{T}}) = \frac{2\eta E}{(1-\nu)}\left[-\varphi + \frac{1}{L}\int_{-L/2}^{L/2} \varphi dz\right] + \frac{F_x}{A} \tag{21}$$

$$tr(\underline{\underline{T}}) = \frac{2\eta E}{(1-\nu)}\left[-\varphi + \frac{1}{L}\int_{-L/2}^{L/2} \varphi dz\right] - \frac{\eta E}{L}\int_{-L/2}^{L/2} \varphi dz + EE_x^{TOT} \tag{22}$$

while the expressions for the mass flux remain unaltered. The boundary conditions

Copyright © 2007 WILEY-VCH Verlag GmbH & Co. KGaA, Weinheim

for eq. 10, assuming instantaneous equilibrium at the polymer-fluid interface, are:

$$\mu^F(P,T) = \mu(\underline{\underline{T}},\varphi) = \mu(\underline{\underline{0}},\varphi) - \eta \cdot V_1 \cdot tr(\underline{\underline{T}}) \quad at\ z = \pm L/2 \tag{23}$$

where $\mu^F(P,T)$ is the chemical potential of the solute in the external reservoir at pressure P and temperature T. It is worth noting that these are time-dependent boundary conditions in view of the time-dependence of $tr(\underline{\underline{T}})$. In summary, if the effect of stresses accompanying the diffusion process is significant, the one-dimensional sorption problem in a thin film can be simply solved by using a differential mass balance containing an effective diffusivity (whose value depends upon elastic constants of the material), with associated time-dependent boundary conditions.

In Figure 4 are compared the mass uptakes vs the square root of sorption time for an unloaded film and for a film submitted to a 7N tensile load (equivalent to a stress of 22.5 MPa). The kinetics were detected by on-line FTIR in terms of absorbance area in the OH stretching region and have been converted into grams of water per 100 grams of polymer by using the molar absorptivity values for water species. A sigmoidal shape can be detected in both cases. This indicates that the effect of self-stress is of some importance in the case of free-standing film. In fact an ideal Fickian behavior would imply a linear increase, at short times, of the sorbed amount as a function of square root of time. The effect of tensile stress on the chemical potential determines an increase of solubility in the loaded sample as compared to the unloaded sample, as expected on the basis of eq. 23. The comparison of sorption kinetics in normalized form (i.e. reporting the time evolution of the ratio $M(t)/M_\infty$, where M(t) and M_∞ are, respectively, the total mass of solute sorbed at time t and at sorption equilibrium), shows that the kinetics in the two case are undistinguishable (see Figure 5). On the basis of the linear Larchè-Cahn theory this is to be expected since the mass flux expression is exactly the same in both cases and the only effect on the boundary conditions of the presence of a tensile load consists in an additive constant term (i.e.$-\eta V_1 \frac{F_x}{A}$). Partially similar arguments can be used to comment on the results for sorption kinetics of films submitted to a constant total tensile deformation (3.8% and 5.7%) during water sorption (see Figures 6 and 7). It is worth noting that (see Figure 7) the films submitted to a constant total deformation display a sorption kinetics which is faster than for unloaded film. Also this feature can be rationalized in the framework of the Larchè-Cahn model by considering that

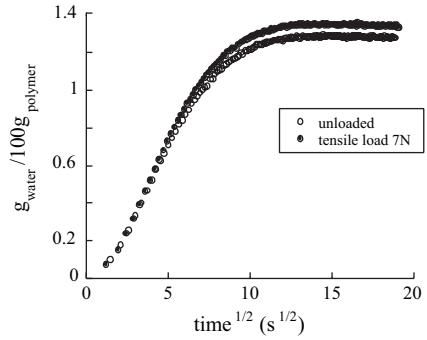

Figure 4.
Sorption kinetcs for unloaded and loaded PMDA-ODA thin films.

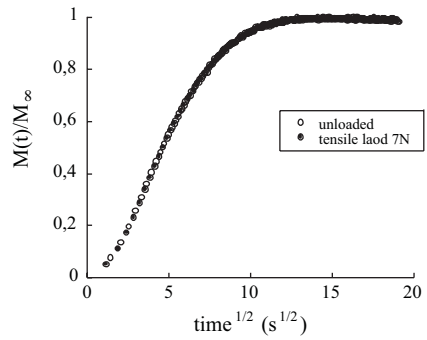

Figure 5.
Normalized sorption kinetcs for unloaded and loaded PMDA-ODA thin films.

Copyright © 2007 WILEY-VCH Verlag GmbH & Co. KGaA, Weinheim

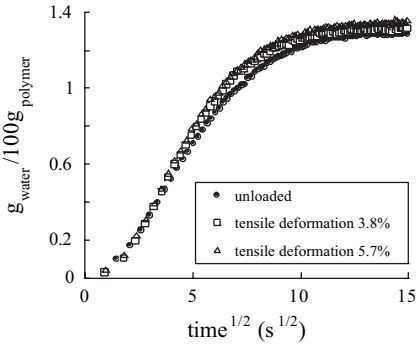

Figure 6.
Sorption kinetcs for unloaded and deformed PMDA-ODA thin films.

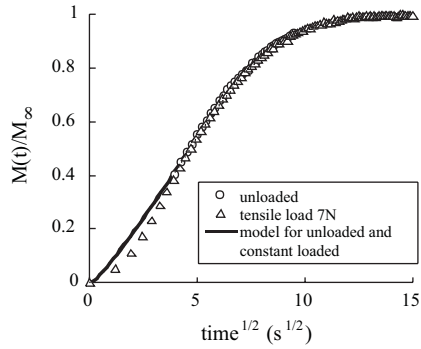

Figure 8.
Experimental data and model prediction for unloaded and loaded thin films.

in the $tr(\underline{\underline{T}})$ now appears, besides an additive constant term, *EExTOT*, also an additive time-dependent term, i.e. $-\frac{\eta E}{L}\int_{-L/2}^{L/2}\varphi dz$. This determines an additive time dependency in the boundary conditions, as compared to the unloaded case. Simulations of water sorption in thin polyimide films for the unloaded, constant load and constant deformation cases have been obtained adopting the Larchè-Cahn linearized theory, by solving numerically equation 10, with symmetric boundary conditions given by eq. 23 and using the proper expressions for $tr\left(\underline{\underline{T}}\right)$ and J_z (see eqs. 18, 21 and 22 for $tr\left(\underline{\underline{T}}\right)$ and eq. 20 for J_z). A fitting of sorption kinetics data with the model equations has been performed contemporaneously at the four different experimental conditions: 1) unloaded film, 2) film submitted to a 7N tensile load, 3) film submitted to a constant total tensile deformation equal to 3.8% and 4) to a constant total tensile deformation equal to 5.7%. η and D have been used as fitting parameters, while all the other parameters have either been determined by independent experiments or obtained from the literature: $\mu(\underline{0},\varphi)$ has been obtained from the sorption isotherm determined gravimetrically, E has been obtained from mechanical tests (2.9 GPa), ν has been taken as equal to 0.33 and, for the partial molar volume of water (V_1), a constant value equal to $18\cdot10^{-6}$ m^3/mole has been used. The results of the fitting are reported in Figures 8 and 9. The model captures the

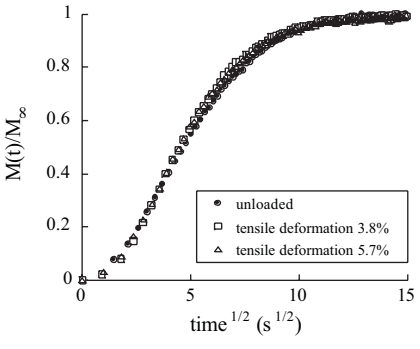

Figure 7.
Normalized sorption kinetcs for unloaded and deformed PMDA-ODA thin films.

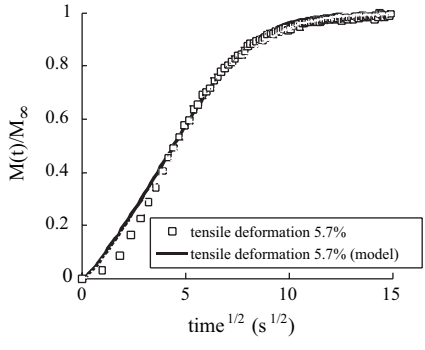

Figure 9.
Comparison of experimental data and model prediction for unloaded and deformed thin films.

Copyright © 2007 WILEY-VCH Verlag GmbH & Co. KGaA, Weinheim

relevant experimental features, although some mismatch with data is evident at short times, likely due to the simplifying assumptions that have been made, the most relevant being the independence of η and V_1 on concentration. Neglecting viscoelastic and plastic effects is, instead, considered appropriate in view of the high glass transition temperature of the polymer and of the small loading levels. From the fitting procedure we obtained for η and D, respectively, the values of 0.53 and $1.6 \cdot 10^{-8}$ cm^2/s.

[1] C. L. Soles, F. T. Chang, B. A. Bolan, H. A. Hristov, D. W. Gidley, and A. F. Yee, *J. Pol. Sci., Part B Pol. Phys.* **1998**, *36*, 30.
[2] C. Grave, I. McEwan, and R. A. Pethrick, *J. Appl. Pol. Sci.* **1998**, *69*, 2369.
[3] J. Mijovic, N. Miura, H. Zhang, and Y. Duan, *J. Adhesion Sci.* **2001**, *77*, 323.
[4] S. Cotugno, G. Mensitieri, P. Musto, and L. Sanguigno, *Macromolecules* **2005**, *38*, 801.
[5] C. M. Huggins, G. C. Pimentel, *J. Phys. Chem.* **1956**, *60*, 1615.
[6] P. Mirone, G. F. Fabbri, *Gazz. Chim. Ital.* **1956**, *86*, 1079.
[7] P. Musto, G. Ragosta, L. Mascia, *Chem. Mater.* **2000**, *12*, 1331.
[8] P. Musto, G. Ragosta, G. Scarinzi, L. Mascia, *J. Pol. Sci.: Part B: Pol. Phys. Ed.* **2002**, *40*, 922.
[9] J. Crank, in: "*The Mathematics of Diffusion*". 2nd ed., Clarendon Press, Oxford 1975.
[10] F. C. Larché, and J. W. Cahn, *Acta Metallurgica* **1982**, *30*, 1835.
[11] P. Neogi, M. Kim, and Y. Yang, *AIChE Journal* **1986**, *32*(7), 1146.
[12] F. Larchè, and J.W. Cahn, *Acta Metallurgica* **1973**, *21*, 1051.
[13] M. Kim, and P. Neogi, *J. Appl. Pol. Sci.* **1984**, *29*, 731.

Copyright © 2007 WILEY-VCH Verlag GmbH & Co. KGaA, Weinheim